RESTRICTED TRANSPORT IN SMALL PORES

A MODEL FOR STERIC EXCLUSION AND HINDERED PARTICLE MOTION

JOHN L. ANDERSON *and* JOHN A. QUINN

From the School of Chemical Engineering, Cornell University, Ithaca, New York 14850 and the School of Chemical and Biochemical Engineering, University of Pennsylvania Philadelphia, Pennsylvania 19174

ABSTRACT The basic hydrodynamic equations governing transport in submicron pores are reexamined. Conditions necessary for a simplified, one-dimensional treatment of the diffusion/convection process are established. Steric restrictions and Brownian motion are incorporated directly into the resulting model. Currently available fluid mechanical results are used to evaluate an upper limit on hindered diffusion; this limit is valid for small particle-to-pore ratios. Extensions of the analysis are shown to depend on numerical solutions of the related hydrodynamic problem, that of asymmetrical particle motion in a bounded fluid.

INTRODUCTION

The simplest conceptual model for a selective diffusion barrier is that of a porous membrane. Relative membrane permeability is measured by comparing solute diffusivity (D) within a pore to that in the bulk solution (D_∞), with $\xi \equiv D/D_\infty$. For nonelectrolytes diffusing through neutral pores ξ is a function of the relative size of permeant and pore, λ, as well as shape. For a rigid, spherical solute (radius a) and circular pore (radius r_0), $\lambda = a/r_0$; if $\lambda > 1$, the membrane is obviously impermeable. However, through steric as well as hydrodynamic factors the presence of the pore wall can significantly hinder movement through the pore for $\lambda < 1$. In fact, our model suggests that for $\lambda = 0.1$, ξ is less than 0.6.

The description of membrane transport in terms of a series of parallel pores has received considerable attention over the years. The current state of development is summarized in two comprehensive reviews: Solomon (1) examines the overall problem of characterizing biological membranes by way of equivalent pores, and Bean (2), in a far-reaching analysis of the physics of porous membranes, considers the theoretical foundation for treating porous membrane transport phenomena and advances existing theory in several important ways. Earlier publications by Pappenheimer, Renkin, and Borrero (3), by Pappenheimer (4), and by Renkin (5) have had a considerable impact on studies in this area, and much of the current research stems from these key papers. A major experimental development which has heightened interest in transport through pores has been the fabrication of model pores of near molecular dimension by the track-etch process (6, 7). Here, for the first time, porous membranes of precisely known dimensions and properties are available for testing predictions of transport theory and for exploring phenomena peculiar to molecular size pores. Important advances have been achieved with these membranes and they should feature prominently in future experimental work.

In this paper we consider a model for pore diffusion based on hydrodynamic relations valid for so-called "creeping flow," while incorporating pertinent characteristics of Brownian motion. The model is first developed for a spherical, diffusing particle for which the computed results of Famularo (8) and Hirschfeld (9) are used to calculate the degree of hindrance. Extensions of the model for nonspherical particles, in the form of explicit but incalculable (due to presently unknown parameter values) expressions, are then presented. The formulation of Giddings et al. (10) is used to account for steric effects. Results are compared with recent experimental findings and classical molecular friction models (11), and implications to membrane characterization are discussed.

BASIC ASSUMPTIONS

The geometry of the liquid-filled pore is shown in Fig. 1. The cylindrical pore has length l and radius r_0. The impenetrable pore wall is assumed inert, i.e., no adsorption or chemical reactions occur, and solvent fluid properties within the pore are assumed identical to those in the bulk (12). Electrical double layer effects are assumed negligible by virtue of either a small wall charge or the presence of a supporting electrolyte in the solvent.

The permeating solute molecule (or particle) is assumed rigid and to possess both hydrodynamic and Brownian characteristics. A hydrodynamic concept of molecular motion is the basis for many of the prominent theoretical developments for diffusion (1, 2, 13–15) and is embodied in Einstein's equation (16):

$$D_\infty = kT/f_\infty, \tag{1}$$

where f_∞ is the molecular friction coefficient computed for a steady Stokes flow ($6\pi\eta a$ for a sphere, η equaling the solvent viscosity) and D_∞ the diffusivity in an unbounded fluid. This relation has been found to accurately predict the diffusivity of globular proteins ($a \sim 30$ Å) and 450 Å latex particles (17, 18), as well as being a good approximation for the behavior of molecules as small as glucose (19). The Wilke-Chang correlation (20) for binary diffusivities is equivalent to Eq. 1 if the solute radius exceeds two or three times that of the solvent. In essence then the solvent must appear as a continuous fluid phase as viewed by the diffusing solute for the latter to be treated as a macroscopic Stokes particle.

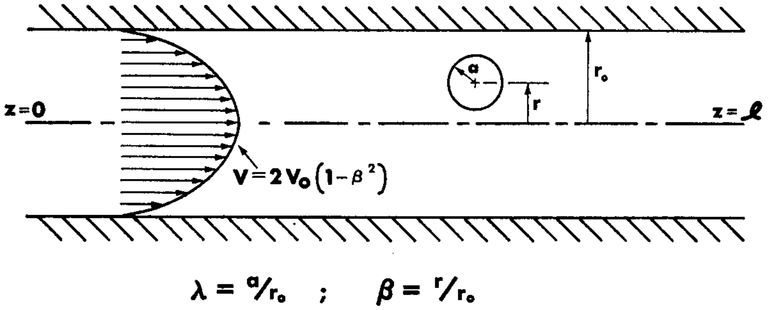

FIGURE 1 Particle located off the centerline of a long, cylindrical pore with a parabolic velocity profile.

Besides attributing hydrodynamic properties to the diffusing molecule, Einstein assumed in deriving Eq. 1 that the gradient in chemical potential at low concentrations manifests itself as a net body force which results in solute transport. The short time Brownian fluctuations normal to the direction of transport are neglected in computing the viscous solute-solvent drag (see note 6 in ref. 16). This concept of chemical potential acting as a mechanical force on a molecular scale is discussed by Gosting (21) and Bearman (22).

The Brownian nature of the solute causes several deviations from macroscopic analyses in describing transport within small pores. Rotational diffusion opposes molecule (particle) alignment in a shear field. Thus molecular orientation and position with respect to the pore axis tend to be randomized rather than exhibiting the orbitals observed for nonspherical macroscopic particles (23). Because of this randomization, the wall effect on the solute-solvent frictional interaction must be averaged over all orientations and radial positions allowed within the pore. Such averaging has been neglected in all previous analyses of pore transport, with the exception of the recent work by Bean (2).

SPHERICAL PARTICLES

Solute-solute interactions within the pore are small compared with wall effects if the following inequality holds (see ref. 8, p. 361):

$$\phi < 2\lambda/3, \tag{2}$$

where ϕ is the solute volume fraction in the pore (based on pore volume) and λ its dimensionless size (a/r_0). An undisturbed Poiseuille flow field should then describe the velocity in the solvent phase:

$$V = 2V_0(1 - \beta^2). \tag{3}$$

β is the dimensionless radial position r/r_0 of the center of the solute molecule, and V_0 equals the average velocity as defined by the total volume flow rate through one pore (solvent + solute) divided by the pore cross-section. A one-dimensional model for mass transfer results from balancing the driving force for the solute flux ($-\nabla\mu$) with the drag (F_s) between solute and solvent; expressing the chemical potential in terms of solute concentration (unit activity coefficient assumed) yields

$$-kT\frac{\mathrm{d}\ln C}{\mathrm{d}z} = F_s \tag{4}$$

Defining U_s as the net solute velocity with respect to the pore wall, the drag on each solute molecule is given by[1]

$$F_s = f_\infty K[U_s - GV], \tag{5}$$

where the "enhanced friction" K (ratio of pore-to-bulk friction coefficients) and the "lag coefficient" G account for the retarding effect of the pore wall on the solute velocity. By combining Eqs. 1, 4, and 5 and substituting the axial solute flux, $N_s = CU_s$, the following results:

$$N_s = -K^{-1}D_\infty\frac{\mathrm{d}C}{\mathrm{d}z} + GCV. \tag{6}$$

The reciprocal of the enhanced friction, K^{-1}, is the *local* ratio of pore-to-bulk solute diffusivity, while G determines the degree to which the solute lags the fluid approach velocity (i.e., V is evaluated by Eq. 3). Both parameters approach unity as an upper limit for large pores ($\lambda \rightarrow 0$).

Both the pore diffusivity and the lag coefficient are functions not only of solute size but also radial position; therefore, the flux of solute will vary with β. The concentration is assumed to be only a function of z (discussion of this assumption follows), so Eq. 6 may be integrated along with Eq. 3 over the pore cross-section to arrive at an average solute flux (moles per square centimeter per second) through one pore:

$$\bar{N}_s = -\xi D_\infty\frac{\mathrm{d}C}{\mathrm{d}z} + \chi C V_0 \tag{7}$$

$$\xi \equiv \frac{D}{D_\infty} = \int_0^{1-\lambda}[2\beta K^{-1}]\,\mathrm{d}\beta \tag{7a}$$

$$\chi = \int_0^{1-\lambda}[4\beta(1-\beta^2)G]\,\mathrm{d}\beta. \tag{7b}$$

---

[1] The small degree of translational-rotational coupling of motion (24, 25), which occurs even for spherical particles when very near surfaces, is neglected. Eq. 5 results from solving the creeping flow form of the Navier-Stokes equation (8, 26–28) and was first applied to molecular transport phenomena by Bean (2).

ξ is the observed ratio of pore-to-bulk solute diffusivity (based on bulk concentration differences) and χ is the sieving coefficient. The upper limit of integration in Eqs. 7 *a* and 7 *b* results because the center of the spherical molecule cannot approach the pore wall any closer than its radius *a*, and hence the real transport area is smaller than the pore area. Because solute concentration is determined by the volume available to the center of the spheres, but defined by the total pore volume, this limit $(1 - \lambda)$ is equivalent in interpretation to defining a steric partitioning coefficient (Φ) for solute between pore and bulk fluid for a spherical molecule as first suggested on geometric grounds by Ferry (29) and later derived from thermodynamic arguments by Giddings et al. (10):

$$\Phi = (1 - \lambda)^2. \tag{8}$$

The pore diffusivity and sieving may then be expressed in terms of the product of this coefficient and the average of the coefficients K^{-1} and G over the available pore area:

$$\xi = \Phi\overline{K^{-1}}(\lambda) \tag{8 a}$$

$$\chi = \Phi[2 - \Phi]\bar{G}(\lambda), \tag{8 b}$$

where the integral formulas for the averaged hydrodynamic parameters $\overline{K^{-1}}$ and $\bar{G}$ are directly obtained from Eqs. 7 *a* and 7 *b*:

$$\overline{K^{-1}} = \frac{\int_0^{1-\lambda} [2\beta K^{-1}]\, d\beta}{\int_0^{1-\lambda} 2\beta\, d\beta} \tag{8 c}$$

$$\bar{G} = \frac{\int_0^{1-\lambda} [4\beta(1 - \beta^2)G]\, d\beta}{\int_0^{1-\lambda} 4\beta(1 - \beta^2)\, d\beta}. \tag{8 d}$$

The extra factor $(2 - \Phi)$ in Eq. 8 *b* accounts for the parabolic velocity profile in the pore.

To account for a finite solvent size in partitioning it has been the practice (1) to divide the right-hand side of Eqs. 8 *a* and 8 *b* by $(1 - \lambda^*)^2$ and $(1 - \lambda^*)^2$ $[2 - (1 - \lambda^*)^2]$, respectively, where λ^* is the ratio of solvent-to-pore radius. This correction simultaneously invokes a hard sphere molecular model for the solvent as well as continuum principles (i.e., negligibly small solvent size) embodied in the hydrodynamic factors, two mutually exclusive concepts. Although the pore-bulk partition coefficient is perhaps adequately corrected for finite solvent dimension by dividing Eq. 8 by $(1 - \lambda^*)^2$, the practice of using the continuum based parameters K and G to estimate hindered transport in such a system is of questionable validity.

Bean (2) recognized the need to average the frictional and lag parameters over available radial positions. However, he directly integrated the coefficient K (F^{-1} in his nomenclature) to obtain

$$\xi_B = \Phi[\bar{K}(\lambda)]^{-1}, \tag{9}$$

a relation which is inconsistent with the definition of K and, therefore, incorrect. If the deviations of K from unity are small for nearly all values of β (i.e., $\lambda \rightarrow 0$), then the differences between Eqs. 8 *a* and 9 are small; however, the error in Eq. 9 may be serious for large values of λ. Since direct integration of Eq. 6 is mathematically consistent with the assumption of negligible variation of concentration with radial position, Eq. 8 *a* should be used to calculate pore diffusivity.

CONDITIONS REQUIRED FOR ONE-DIMENSIONAL TREATMENT

The assumptions of a fully developed Poiseuille flow (in the cylindrical pore) and negligible dependence of concentration on radial position, both of which are necessary to derive Eq. 7 to 7 *b*, are now examined. The axial distance (L_D) from the pore inlet required to establish a fully developed parabolic velocity profile may be calculated from Langhaar's expression (30),

$$L_D/r_0 = (0.115)\, Re, \tag{10}$$

where Re is the Reynolds number for tube flow, $2V_0 r_0 \rho/\eta$, and ρ is the solvent density. For micron-sized aqueous pores with reasonable pressure gradients (less than 10^8 atm cm), the required value of L_D/r_0 is less than 0.3, indicating that the velocity profile is essentially fully developed at the pore inlet.

Although no solute (nor solvent) can diffuse through the pore wall, the possibility of radial concentration gradients still exists due to the nonuniform fluid velocity. In fact, it is this radial transport which causes the axial dispersion so important in reacting systems. Criteria which must be met to apply a one-dimensional model of transport to convection-diffusion systems are extensively reviewed by Levenspiel and Bischoff (31). Although the analyses are for time-dependent (pulsed) systems, the results are assumed to hold true for the steady-state form of the mass flux equation. The approximate criterion for the validity of a one-dimensional model as used here is given by

$$l/r_0 > Pe^{1/2}, \tag{11}$$

where the axial Peclet number (Pe) equals $\chi V_r l/\xi D_\infty$). Thus, if Pe is less than 10, the transport in a pore whose length-to-diameter ratio is greater than two is properly modeled by a one-dimensional analysis and Eq. 7 is valid.[2]

At higher Peclet numbers convection dominates the solute transport. If C is assumed to be independent of β (or it represents a concentration averaged over the pore cross-section), the solution to Eq. 7 is

$$\frac{C(\zeta)}{C_0} = \frac{(C_1/C_0)[e^{Pe\zeta} - 1] + e^{Pe}[1 - e^{-Pe(1-\zeta)}]}{(e^{Pe} - 1)}, \tag{12}$$

where ζ is the dimensionless axial position (z/l), C_0 and C_1 are the bulk concentrations at ζ equal to zero and one, respectively. Eq. 12 with $C_1 = 0$ is plotted in Fig. 2 for different values of Pe. An immediate observation is that for $Pe > 10$ the concentration profile is very flat, C remaining essentially equal to C_0 for at least the first half of the pore length. Because C is truly independent of radial position at $\zeta = 0$ (and at $\zeta = 1$) if no significant boundary layer resistances exist exterior to the membrane, then C will remain nearly independent of β for $\zeta < \frac{1}{2}$. Because the average solute flux ($\bar{N}_s$) is a constant, it may be computed at any axial position; thus, the best choice is at $\zeta = 0$ for large Pe systems, where axial concentration gradients (and hence diffusion) are negligible:

$$\bar{N}_s \doteq \chi C_0 V_0 . \tag{13}$$

(It should be noted, however, that in this case C may depend on β near the end of the pore where axial gradients are largest, and hence Eq. 12 may not accurately describe the concentration profile in the whole pore.) It is concluded that a one-dimensional convection-diffusion model of solute transport is valid for calculating $\bar{N}_s$ even at large Pe. The general expression for solute flux is found by substituting Eq. 12 into Eq. 7:

$$\bar{N}_s = \chi C_0 V_0 \frac{[1 - (C_1/C_0)e^{-Pe}]}{[1 - e^{-Pe}]}. \tag{14}$$

STERIC FACTORS

A few remarks about steric partitioning are in order. Giddings et al. (10) argue that the physical pore concentration C_p based upon the total pore volume is less than the bulk value because of the geometric restriction on the solute approach to the pore wall. For a rigid particle (molecule) of dimension λ and shape ϵ (long-to-short dimension) they derive the following configurational integral which determines partitioning:

$$C_p/C = \Phi = \int_{\text{all } \Psi} \int_0^1 2\beta P_s(\lambda, \epsilon; \beta, \Psi)\, d\beta\, d\Psi, \tag{15}$$

---

[2] The effective axial diffusion coefficient would be $D[1 + (Pe^2/48)(r_0/l)^2]$. Since the quantity $Pe(r_0/l)^2 < 1$ by Eq. 11, then $D_{\text{eff}} = D = \xi D_\infty$ except when $Pe \gg 1$, in which case diffusion of solute is unimportant in contrast to the convective flux.

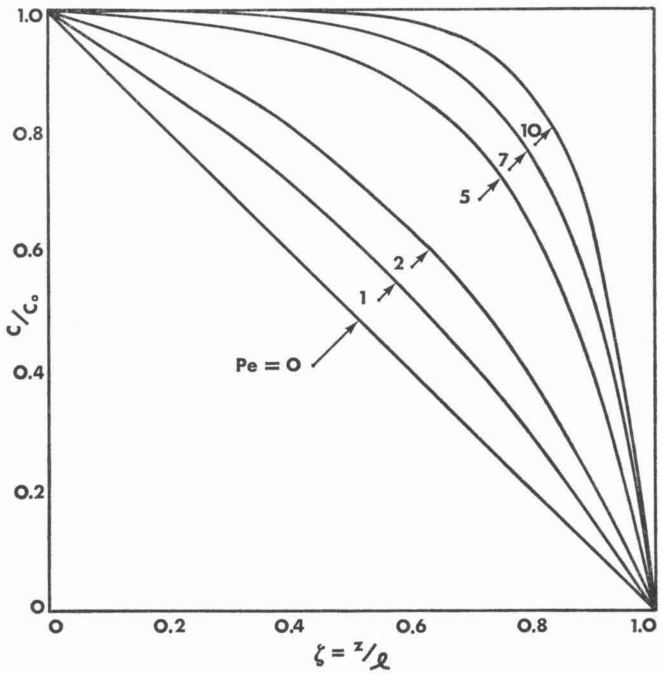

FIGURE 2 Dimensionless concentration versus dimensionless axial position for various Peclet numbers (calculated from Eq. 12 for zero exit concentration, $C_1 = 0$).

where Ψ represents the Eulerian angular orientation[8] of the particle with respect to the pore axis, and P_s is a discrete probability which equals 1 if the particle can be situated within the pore (without penetrating the pore wall) with the given variables, and zero otherwise. For spherical molecules orientation and shape effects are absent and Eq. 8 results. Our derivations of ξ and χ for spherical molecules essentially incorporate Eq. 15 directly (in the limits of integration), so that C appearing in Eqs. 7 and 14 is identical to the bulk concentration at equilibrium since it is based only on the *available* pore volume. That is to say C_0 and C_1 in Eq. 14 are the *bulk* solute concentrations on each side of the membrane. We are unaware of any conclusive experimental findings which prove that pore concentration based on available volume equals the bulk value at equilibrium, and thus it is accepted here on the strength of the arguments of Giddings et al. (The results of Satterfield et al. [32] suggest that perhaps this point requires further investigation.)

RESULTS BASED ON HYDRODYNAMIC CALCULATIONS

The values of K^{-1} and G necessary for evaluation of Eqs. 7 *a* and 7 *b* can be taken in principle from the calculations for the friction and lag of a sphere in a long cylin-

---

[8] Ψ is normalized such that $\int_{\text{all } \Psi} d\Psi = 1$. See Happel and Brenner, p. 205 (8).

drical tube under Stokes flow conditions. A review of current progress in performing these calculations is summarized by Brenner and co-workers (8, 26). Results for spheres whose centers are restricted to the centerline axis of the tube are available for $\lambda \leq 0.99$ (27, 33) and the following are good approximations for $\lambda < 0.4$:

$$K^{-1}(\lambda, 0) \doteq 1 - 2.1044\,\lambda + 2.089\,\lambda^3 - 0.948\,\lambda^5 \tag{16 a}$$

$$G(\lambda, 0) = 1 - \tfrac{2}{3}\lambda^2 - 0.163\,\lambda^3. \tag{16 b}$$

If it is assumed that $K^{-1}(\lambda, 0)$ and $G(\lambda, 0)$ are accurate approximations to the radially-averaged K^{-1} and velocity-averaged G, then Eqs. 8 *a* and 8 *b* may be used to derive the so-called "centerline approximation" for the hindered diffusivity and sieving coefficient:

$$\xi \approx \xi_0 = (1 - \lambda)^2 K^{-1}(\lambda, 0). \tag{17 a}$$

$$\chi \approx \chi_0 = (1 - \lambda)^2[2 - (1 - \lambda)^2]G(\lambda, 0). \tag{17 b}$$

Eq. 17 *a* was originally derived by Pappenheimer and co-workers (3–5) and has been the subject of considerable experimental investigation (1, 2, 5, 18, 32, 34, 35]. To estimate sieving effects Renkin (5) incorrectly assumed $G = K^{-1}$ (as Bean emphasizes [2]) in Eq. 7 *b* to obtain the following expression for sieving:

$$\chi_R = (1 - \lambda)^2[2 - (1 - \lambda)^2]K^{-1}(\lambda, 0). \tag{18}$$

However, the friction coefficient K is considerably greater than $1/G$. The error in using Eq. 18 may be considerable as is apparent from Fig. 3 which plots calculations from Eqs. 17 *a*, 17 *b*, and 18.

The dependence of the hydrodynamic parameters on off-centerline position for spherical particles is not completely known. Famularo (8) and later Hirschfeld (9) generated numerical solutions for a function $f(\beta)$ relating the effect of eccentric position on the hindrance of small particles at zero volume flow:

$$K^{-1} = 1 - f(\beta)\lambda \pm 0\left[\frac{\lambda^3}{(1 - \beta)^3}\right]. \tag{19}$$

The values of $f(\beta)$ are in tabular form but are approximated quite well by

$$f(\beta) \doteq 2.09 \qquad \beta < 0.6$$

$$f(\beta) \doteq \tfrac{9}{16}(1 - \beta)^{-1} + 1.9(1 - \beta) \qquad 0.6 \leq \beta < 1. \tag{20}$$

Eq. 19 has apparently been used by Bean (2) to evaluate $\bar{K}$ for substitution into Eq. 9. Besides the previously mentioned inconsistency in his averaging technique, two quite important limitations on $f(\beta)$ seem to have been overlooked. First, Eq. 19

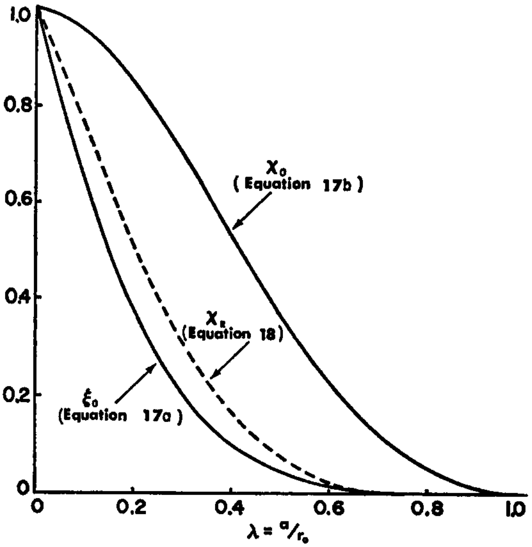

FIGURE 3 Pore retardation of solute diffusion and convection as predicted from centerline values of the hydrodynamic parameters.

is correct only to order λ, so its validity is probably only assured for, say, $\lambda < 0.1$. The second limitation is perhaps more important: the numerical results of Famularo and Hirschfeld are only valid for $\beta \ll (1 - \lambda)$. Because the greatest hindrance is experienced near the pore wall ($\beta \sim 1 - \lambda$) and the fractional pore area is greatest at this location, this restriction on $f(\beta)$ severely limits the usefulness of Eq. 19. Since the error of employing only the leading term is of order $(\lambda/[1 - \beta])^3$, then it is probably unwise to use this correction when the particle center is closer than two or three radii from the pore wall.

A composite formula utilizing both cylindrical tube and flat wall calculations for increased drag perhaps offers a more reliable method of computing the average coefficient $\overline{K^{-1}}$. Restricting the analysis to $\lambda \leq 0.1$, let K^{-1} be given by Eq. 19 for $\beta \leq \beta\ddagger$ and by K_w^{-1} for $\beta\ddagger < \beta \leq 1 - \lambda$, where the latter is the inverse enhanced friction for a sphere translating parallel to an infinite, flat wall (24).[4] The average coefficient is then approximated as

$$\xi = (1 - \lambda^2)\overline{K^{-1}} \simeq \int_0^{\beta\ddagger} 2\beta[1 - f(\beta)\lambda]\, d\beta + \int_{\beta\ddagger}^{1-\lambda} [2\beta K_w^{-1}]\, d\beta. \qquad (21)$$

If $\beta\ddagger$ is set equal to $1 - 2\lambda$, then it is easily shown that K_w^{-1} nearly equals the calculation from Eq. 19 at this point and a continuity is achieved in the composite formula. One must remember, however, that the error in using Eq. 19 even at $\beta = 1 - 2\lambda$

---

[4] As mentioned earlier, rotational-translational coupling of motion is negligible for all but (perhaps) very eccentric particles. In the article by Goldman et al. (24) their $-F_x^{t*}$ corresponds to our K_w and their $(-F_x^{s*}/F_x^{t*})$ to our G_w.

is of order $\frac{1}{8}$ in K^{-1}. The rationale for using this particular formula derives from the fact that $[1 - f(\beta)\lambda]$ approaches K_w^{-1} to the first power in λ as $\beta \rightarrow 1$ (8), which implies that at least for small particles ($\lambda \ll 1$) the pore wall curvature is of second order importance. Use of the flat wall model to approximate the increased resistance for $\beta \rightarrow (1 - \lambda)$ leads, of course, to an underestimate of the retardation for finite λ, but it does yield the correct point value $K^{-1} = 0$ when the particle touches the pore wall (24). Calculations based on Eq. 21 are plotted in Fig. 4; shown for comparison is the centerline estimate with only terms up to the first power in $K^{-1}(\lambda, 0)$ included.

Because the accuracy of Eq. 21 is somewhat suspect for $\lambda > 0.1$, it would serve no useful purpose to extend the calculations to larger λ. Lubrication theory has been attempted by Bungay (33) to determine the resistance experienced as $\beta \rightarrow 1 - \lambda$, but the results are not quantitatively useful. The retardation should be infinite at particle wall contact ($\beta = 1 - \lambda$), but the variation with β up to this point may not be monotonic. The statement that the centerline approximation is valid as $\lambda \rightarrow 1$ is, of course, true since it predicts a zero pore diffusivity in the limit, but the asymptotic approach may not be correct.

Experiments attempting to measure D/D_∞ for a significant range of λ are summarized by Solomon (1) and Bean (2). Uzelac and Cussler (35) measured the diffusion of uniform, spherical latex particles ($a \sim 450$ Å) through small pores in Millipore filters (Millipore Corp., Bedford, Mass.); however, unknown complications seem

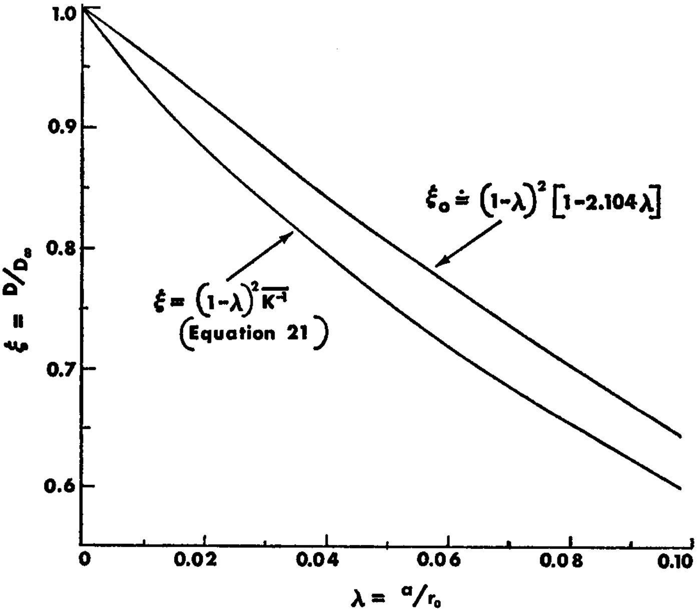

FIGURE 4 Comparison of the hindered diffusion as predicted from the centerline friction (ξ_0) and from the radially-averaged friction (ξ) for small particles.

to have clouded their results (36). Recently Conlon and Craven (18) published results for the hindered diffusion of spherical lattices through track-etched pores, but their values of D/D_∞ lie well above even the centerline approximation (Eq. 17 *a*). Satterfield et al. (32) found that the wall retardation to diffusion of small molecules in aqueous pores within silica-alumina beads is significantly greater than predicted by the centerline approximation. Their results also indicate that the pore-bulk partitioning (Φ) is unity. Beck and Schultz (34) have performed what are perhaps the most precise experiments to date for determining D/D_∞ ; the pores in their membranes were long and approximately cylindrical with no tortuosity, and the pore size distribution was quite narrow. Although their data scatter to some extent, many of the points lie below Eq. 17 *a*, and for $\lambda < 0.1$ the data show fair agreement with the calculations derived from averaging the retarding effect over the available pore cross-section (lower curve of Fig. 4). Most of the solutes studied by Beck and Schultz were not much larger than the solvent (water), so that a hydrodynamic model for hindrance may not be completely valid.

The first correction term for the lag coefficient is of order λ^2. The following is given by Brenner and Bungay (26) for small spherical particles:

$$G = 1 - [\tfrac{2}{3}\lambda^2/(1 - \beta^2)] \pm 0(\lambda^3), \qquad (22)$$

where again the restriction $\beta \ll 1 - \lambda$ is imposed. Since λ must be small, the magnitude of the correction is also small. Because of this second order dependence on λ (see Fig. 3), the sieving becomes significant only when $\lambda > 0.1$, so that substitution of Eq. 22 into the integral 7 *b* would result in only a negligible correction (with respect to absolute magnitude) to the centerline approximation χ_0. This state of affairs is unfortunate since sieving (ultrafiltration) finds much application in separation and purification processes in both laboratory and industrial operations. Often a model consisting simply of completely free passage ($\chi = 1$) or complete rejection ($\chi = 0$) is adopted to describe porous filtration (37), although Fig. 3 indicates no such sharp cut-off. When and if calculations for $G(\beta)$ become available, direct substitution into Eq. 7 *b* should give the correct value of χ; until such a time (or reliable data become available) the centerline approximation (Fig. 3) must suffice as an upper limit to its estimate.

COMPARISON WITH THE FRICTIONAL MODEL FOR COEFFICIENTS ARISING FROM IRREVERSIBLE THERMODYNAMICS

Although only valid at extremely small (convective) driving forces, the integrated form of the coupled equations for total and relative velocities is often used to model membrane transport (38). The more accurate, differential approach is presented by Spiegler and Kedem (11) for a two component solution plus membrane. Their equation for the solute flux is equivalent to Eq. 7:

$$\bar{N}_s = -\frac{\bar{P}}{\alpha}\frac{\mathrm{d}C}{\mathrm{d}z} + (1 - \sigma)CV_0. \tag{23}$$

(To base the flux on the total membrane area rather than just the pore area, multiply $\bar{N}_s$ by the pore area fraction (α), which is equivalent to the water volume fraction in the membrane in our model.) The parameter σ is the classical reflection coefficient (39),

$$\sigma = (\Delta P/RT\Delta C)_{V_0=0}\,, \tag{24}$$

and equals $1 - \chi$ in our model. The "local solute permeability" $\bar{P}$ corresponds to $\alpha\xi D_\infty$ and is related to the classical solute permeability (for a nonelectrolyte) by

$$\omega \equiv (\alpha\bar{N}_s/RT\Delta C)_{V_0=0} = (\bar{P}/l)/RT. \tag{25}$$

The membrane rejection coefficient (R_m) is defined as $1 - C_1/C_0$ when the effluent concentration C_1 is solely determined by the membrane transport rate: $C_1 = \bar{N}_s/V_0$. From Eq. 14 the following expression, also derived by Spiegler and Kedem (11), is obtained:

$$R_m = \sigma\frac{(1 - e^{-Pe})}{1 - \sigma e^{-Pe}}. \tag{26}$$

At large Peclet numbers (high flow rates) $R_m \rightarrow \sigma$.

Bean (2) very neatly relates the characteristic parameters of irreversible thermodynamics (L_P, σ, ω) with the structurally dependent parameters ξ and χ in a quite successful attempt to rationally compare experimental results from several sources for hindered transport of small solutes in porous membranes. Inconsistencies develop, however, when a direct comparison is made of the hydrodynamic model for cylindrical pores with the general molecular friction model proposed by Spiegler (40):

$$F_i = \sum_j f_{ij}\,[U_i - U_j]. \tag{27}$$

For a two-component solution (solute, s, and solvent, w) in pores within a rigid, inpenetrable membrane matrix, the above equation becomes (11, 41)

$$F_s = (f_{sw} + f_{sm})U_s - f_{sw}U_w \tag{28}$$

$$F_w = (f_{ws} + f_{wm})U_w - f_{ws}U_s \tag{29}$$

$$(C_s f_{sw} = C_w f_{ws})$$

Manipulation of these two expressions, assuming a dilute solute concentration and substituting the gradient in chemical potential for the force, yields (40)

$$1 - \sigma = \frac{\Phi f_{sw}}{f_{sw} + f_{sm}} + \frac{\omega \bar{v}_s}{L_P} \qquad (30a)$$

$$L_P = \alpha \left(\frac{V_0}{\Delta P} \right)_{\Delta C = 0} = \frac{\alpha \bar{v}_w}{l f_{wm} N_a} \qquad (30b)$$

$$\omega = \frac{\alpha \Phi}{l(f_{sw} + f_{sm}) N_a}. \qquad (30c)$$

(N_a is Avogadro's number.) The distinction between α and Φ needs emphasis: α is the volume fraction of solvent in the membrane, while Φ is the solute pore-bulk partition coefficient based on the solvent volume in the membrane. Combination of the above set of equations gives the expression derived by Spiegler and Kedem (11),

$$1 - \sigma = \Phi \left[\frac{f_{sw} + f_{wm}(\bar{v}_s / \bar{v}_w)}{f_{sw} + f_{sm}} \right]. \qquad (31)$$

The hydrodynamically-based parameters for parallel, cylindrical pores can now be directly compared to the pore frictional coefficients f_{ij}. Assuming all pores have the same radius r_0, Poiseuille's equation is used to obtain

$$f_{wm} = (8\ \bar{v}_w \eta)/(N_a r_0^2), \qquad (32)$$

where η is the pure solvent viscosity when the solution is dilute (small corrections to Eq. 32 are available if the solute concentration is finite [27, 28, 42]). The hindered diffusion is directly related to the permeability:

$$\xi = D/D_\infty = \omega/(\alpha/l N_a f_\infty) = \Phi f_\infty/(f_{sw} + f_{sm}). \qquad (33)$$

Substitution of Eqs. 32 and 33 into Eq. 31 gives

$$\chi/\xi = f_{sw}/f_\infty + (8\ \eta \bar{v}_s / N_a f_\infty\ r_0^2). \qquad (34)$$

For a spherical solute the second term on the right may be rewritten (using Stokes equation for f_∞):

$$\chi/\xi = (f_{sw}/f_\infty) + (4\lambda/3)^2. \qquad (35)$$

The usual implication (1, 11, 38, 41), whether intended or not, is that unless the solvent is somehow structurally altered by the presence of the pore wall (see ref. 12), the frictional coefficient between solute and solvent in the pore equals that in the bulk solution. Imposing this equality leads to

$$\chi/\xi = 1 + (4\lambda/3)^2. \qquad (36)$$

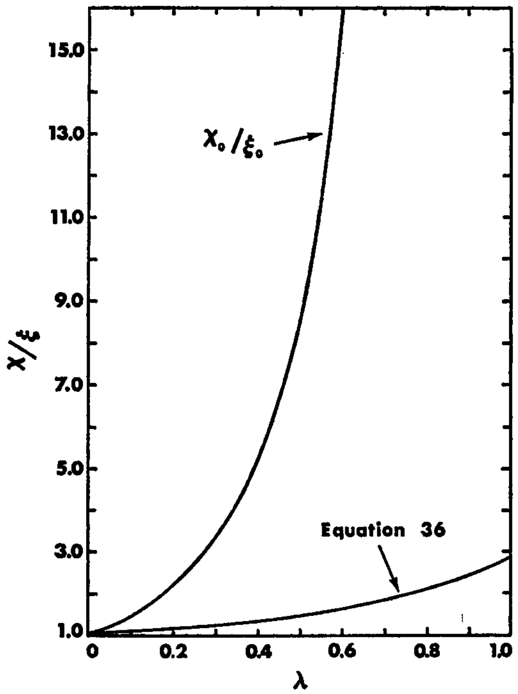

FIGURE 5 The ratio of sieving to hindered diffusion for a spherical solute in a cylindrical pore as predicted from the hydrodynamic theory (χ_0/ξ_0) and from the frictional model of Spiegler (40) (Eq. 36).

From our hydrodynamic model of pore transport the centerline evaluation of both χ and ξ can be used to approximate this ratio:[5]

$$\chi/\xi \approx \chi_0/\xi_0 = [2 - (1 - \lambda)^2][G(\lambda, 0)/K^{-1}(\lambda, 0)]. \qquad (37)$$

The above two equations are plotted in Fig. 5 for comparison. It is evident that the two models do not agree, and hence the so-called general frictional model (Eqs. 28 and 29) is inadequate at least to correctly describe the transport of spherical solutes in cylindrical pores. The fault in this treatment is that in the absence of adsorption there is *no direct frictional interaction between solute and membrane* (see the discussions by Bean (2) and by Dainty and Ginzburg (41) on this point). The hindrance to solute transport in small pores is due to the indirect hydrodynamic effect of the pore wall: the shear stresses (friction) between solute and solvent are increased due to non-slip of the solvent at the pore wall, thereby enhancing f_{sw} above its bulk value f_∞. Thus one should set $f_{sm} = 0$. Conversely, a non-slip condition between solvent and solute increases f_{wm} (42), although the effect is negligible

---

[5] Since ξ_0 is more of an overestimate of ξ than χ_0 is of χ (especially at $\lambda \ll 1$), the ratio χ_0/ξ_0 is an *underestimate* of χ/ξ.

for dilute solute concentrations. These considerations apply not only to parallel, cylindrical pores but also to any heterogeneous membrane in which the solid (fixed) phase is impermeable and inert to both solute and solvent.

A better formulation of the average frictional model for transport through inert porous membranes would be

$$F_s = f_{sw}(U_s - g_{sw}U_w), \tag{38}$$

here f_{sw} and g_{sw} are functions of geometry and size of both pore and solute. The latter coefficient is necessitated by the nonuniform solvent velocity through the membrane interstices. For dilute solutions (i.e., $V_0 \doteq U_w$) the following relations exist:

$$f_{sw} = \Phi f_\infty/\xi; \qquad g_{sw} = \chi/\Phi. \tag{39}$$

It should be noted that at least for cylindrical pores $g_{sw} \geq 1$ because of steric exclusion, that is, the solute molecule actually moves faster than the average velocity of the solvent; however, $\chi < 1$ so that the pore will "filter" the large molecule to some extent. For a homogeneous system in which both solvent and solute dissolve into and diffuse through the membrane matrix, the model of Spiegler (Eqs. 27–29) is preferred since there is direct solute-membrane interaction in this case.

NONSPHERICAL PARTICLES

Orientation becomes a complicating factory in dealing with nonspherical solutes. For ellipsoids the net frictional coefficient between solute and solvent (f_∞) in an unbounded medium is easily calculated by numerically averaging the inverse coefficients for the three principal axes (8, 15). The same molecule in a pore offers problems in that all orientations must be averaged at all radial positions. The mathematical formulation is straightforward, but the information required is formidable.

Assume that rotational Brownian motion is sufficient to ensure complete randomness of solute orientation. Let P_s be the same probability that appears in Eq. 15; again the development of Giddings et al. (10) is followed. The effective radius a is taken as some measure of the size of the molecule, which is assumed to be rigid, and β is the dimensionless radial position of its centroid. The one-dimensional flux equation is still given by Eq. 7, while the pore diffusivity and sieving coefficient are calculated from

$$D/D_\infty = \int_\Psi \int_0^1 [2\beta K^{-1} P_s]\beta \, d\Psi \tag{40a}$$

$$\chi = \int_\Psi \int_0^1 [4\beta(1 - \beta)GP_s]\beta \, d\Psi. \tag{40b}$$

Since P_t can have only two values, its effect can be translated to the limits of integration. Let $\bar{\beta}$ be the radial position at which the molecule first touches the pore wall for a given orientation. Then for $\beta > \bar{\beta}$ the probability is zero and the following may be written:

$$D/D_\infty = \int_\Psi \int_0^{\bar{\beta}(\lambda,\Psi)} [2\beta K^{-1}]\, d\beta\, d\Psi \tag{41 a}$$

$$\chi = \int_\Psi \int_0^{\bar{\beta}(\lambda,\Psi)} [4\beta(1-\beta^2)G]\, d\beta\, d\Psi. \tag{41 b}$$

From such configuration integrals a distribution coefficient can be derived for nonspherical particles:

$$\Phi = \int_\Psi \bar{\beta}^2\, d\Psi \approx (1 - [L/2r_0])^2. \tag{42}$$

The particle modulus L is calculated by Giddings et al. for various shapes and can be thought of as an effective particle diameter.

For a sphere orientation is of no consequence and $\bar{\beta} = 1 - \lambda$, so that the above expressions become equivalent to Eqs. 7 *a* and 7 *b*, with L equaling the particle diameter. In principle knowledge of K^{-1} and G as a function of (λ, β, Ψ) could be substituted into the above integrals for direct evaluation; however, this information is not available. Chen and Skalak (28) have computed these parameters for spheroids with the symmetry axis coincidental with the pore centerline. Happel and Brenner (8) review existing literature which examines the retardation of spheroids moving parallel and normal to flat walls. Because of the mathematical difficulties encountered in asymmetric tube flows, the likelihood that calculations of K^{-1} and G will become available in the near future appears small.

The criterion for randomness of orientation for nonspherical particles is not so general as that for position. Rotational Brownian movement opposes alignment forces caused by the presence of a fluid shear field within the pore; however, randomness is only assured when (43)

$$D_{\text{rot}}/W > 1, \tag{43}$$

where D_{rot} is the rotational diffusivity of the solute and W the vorticity of the velocity field in the pore. If a^* represents one-half the maximum dimension of the solute molecule, then D_{rot} should be greater than $kT/(8\pi\eta a^{*3})$. The vorticity is approximated by V_0/r_0. By substituting for V_0 in terms of pressure drop and pore radius (Poiseuille's equation), the above requirement may be written as

$$a^* < [kT/(\pi r_0 \Delta P/l)]^{1/3}, \tag{44}$$

where $\Delta P/l$ is the pressure gradient within the pore. This expression should be examined to determine whether or not particle alignment along flow streamlines may occur. For example, a pressure gradient of 100 atm/cm in a 1 μm pore requires that the greatest particle dimension be smaller than 200 Å to completely resist alignment. If condition 44 is not met, then the sieving coefficient χ may be a function of not only size and shape but also of volumetric flow rate through the pore.

SUMMARY

The interaction between solute and pore wall in mass transfer through small pores can be characterized in terms of basic fluid mechanical equations. We have shown that a one-dimensional diffusion/convection analysis is valid for microporous systems ($r_0 \leq 1$ μm) which can be approximated by a network of parallel pores. The important result of this one-dimensional simplification is that the pore diffusivity and sieving coefficient can be written explicitly as integrals which appropriately weight the effect of the pore wall on the solute-solvent drag. The proper mean for the frictional resistance results from a direct integration of the local value of D/D_∞ over all allowable radial positions. Pore-bulk partitioning is accounted for by a discrete probability function contained in the above integral; it may be removed to the limit of integration in the case of spherical particles for which orientation is not a variable. Comparison of this transport model with the frictional model of Spiegler and others (11, 38, 40, 41) suggests that the latter may need modifications when applied to a porous membrane. The exact formulas for calculating the extent of hindered transport are Eqs. 7–8 and 40 *a*–40 *b*; however, these equations cannot be evaluated directly since too little is known of $K^{-1}(\lambda, \beta)$ and $G(\lambda, \beta)$ for even spherical particles. For small particle-pore ratios ($\lambda < 0.1$) the lower curve of Fig. 4, which results from averaging the wall effect over radial position, shows a significant correction to the frequently-cited equation of Pappenheimer and co-workers, and our result is but an *upper limit* to the true value. Future analytical advances await further solutions to the hydrodynamic equations for asymmetrical particle motion in a bounded fluid. In addition, precise experimental results are required to substantiate assumptions of the current model and to point the way to further understanding of porous membranes.

LIST OF SYMBOLS

a	Radius of solute molecule (based on a sphere of equivalent volume), cm.
a^*	One-half the greatest dimension of the solute.
C	Pore solute concentration based only on available pore volume (see Eq. 15), mol/cm^3. At each end of the pore we assume C equals the bulk concentration on that side.
C_p	Pore solute concentration based on the total pore volume.
C_0, C_1	Bulk solute concentration at $\zeta = 0$ and 1, respectively.
D	Effective pore diffusivity of solute (based on bulk concentration difference), cm^2/s.
D_∞	Bulk solute diffusivity.

D_{rot}	Rotational diffusion coefficient, s^{-1}.
$f(\beta)$	Function described by Eq. 19.
f_{ij}	Molecular friction coefficient between species i and j, g/(molecule $i \times$ s).
f_∞	Solute frictional coefficient in the bulk solution (function of size and shape of solute).
F_i	Frictional drag force on species i, dyn/molecule.
g_{ij}	Average intermolecular sieve coefficient between species i and j.
$G(\lambda, \epsilon; \beta, \Psi)$	Local lag coefficient between solute and point velocity $V(\beta)$.
$\bar{G}(\lambda, \epsilon)$	Average value of G (Eq. 8 d).
k	Boltzmann's constant, erg/(molecule × °K).
$K(\lambda, \epsilon; \beta, \Psi)$	Local ratio of pore-to-bulk solute friction coefficients.
$K_w(a, r_0 - r)$	f_{sw}/f_∞ for a solute whose centroid is at $r_0 - r$ from an infinite flat wall.
$\bar{K}^{-1}(\lambda, \epsilon)$	Average value of K^{-1}(Eq. 8 c).
$\bar{K}(\lambda, \epsilon)$	Average value of K.
l	Pore length, cm.
L_D	Minimum pore length necessary to establish steady laminar flow, cm.
L_P	Hydraulic coefficient, s × (cm^2/g).
N_a	Avogadro's number, 6.02×10^{23} molecules/mol.
$\underline{N}_s(\beta)$	Local solute flux in the pore, mol/(cm^2 × s).
$\bar{N}_s$	Average of N_s over the pore cross-section (based on pore area).
ΔP	Pressure drop within the pore length, $P(O) - P(l)$, dyn/cm^2.
$\underline{P}_s(\beta, \lambda, \Psi, \epsilon)$	Discrete probability function (Eq. 15).
$\bar{P}$	"Local solute permeability" of Spiegler and Kedem (11), cm^2/s.
Pe	Peclet number, $\chi V_0 l/(\xi D_\infty)$.
r	Radial position in the pore, cm.
r_0	Pore radius.
R	Gas law constant, erg/(mol × °K).
R_m	Membrane rejection.
Re	Reynolds number, $2V_0 r_0 \rho/\eta$.
T	Temperature, °K.
U_i	Velocity of species i with respect to fixed (membrane) coordinates, cm/s.
$\bar{v}_i$	Partial molar volume of species i, cm^3/mol.
$V(\beta)$	Point velocity of solution in the pore, cm/s.
V_0	Average velocity in the pore (total volume flow per pore area).
W	Vorticity of velocity field in pore, s^{-1}.
z	Axial position along pore, cm.
α	Pore area fraction of membrane (or solvent volume fraction).
β	r/r_0.
ϵ	Long-to-short dimension of solute molecule.
ζ	z/l.
η	Solvent viscosity, g/(cm × s).
λ	a/r_0.
λ^*	Ratio of solvent-to-pore radius.
μ	Solute chemical potential, erg per molecule.
ξ	D/D_∞.
ρ	Solvent density, g/cm^3.
σ	Reflection coefficient.
ϕ	Volume fraction of solute in the pore (based on pore volume).

Φ	$(C_p/C)_{\text{equil}}$ = (mol solute/cm^3 pore volume)/(mol solute/cm^3 bulk solution).
χ	Sieving coefficient (Eq. 7 *b*).
Ψ	Eulerian angular representation of solute orientation with respect to pore axis.
ω	Solute permeability, (mol × s)/(cm × g).

Subscripts

s	Solute.
w	Solvent.
0	Centerline ($\beta = 0$) evaluation of K and G used in equations 7 *a* and 7 *b*.

We thank H. Brenner of Carnegie-Mellon University for alerting us to the calculations of B. R. Hirschfeld.

This work was supported in part by research grants from the Office of Saline Water, U. S. Department of the Interior and from the National Science Foundation.

Received for publication 6 April 1973 and in revised form 14 September 1973.

REFERENCES

1. Solomon, A. K. 1968. *J. Gen. Physiol.* **15**:355s.
2. Bean, C. P. 1972. The physics of porous membranes I. *In* Membranes—A Series of Advances. Vol. 1. G. Eisenman, editor. Marcel-Dekker, Inc., New York.
3. Pappenheimer, J. R., E. M. Renkin, and L. M. Borrero. 1951. *Am. J. Physiol.* **167**: 13.
4. Pappenheimer, J. R. 1953. *Physiol. Rev.* **33**:387.
5. Renkin, E. M. 1954. *J. Gen. Physiol.* **38**:225.
6. Quinn, J. A., J. L. Anderson, W. S. Ho, and W. J. Petzny. 1972. *Biophys. J.* **12**:990.
7. Fleischer, R. L., H. W. Alter, S. C. Furman, P. B. Price, and R. M. Walker. 1972. *Science (Wash. D. C.)*. **178**:255.
8. Happel, J., and H. Brenner. 1965. Low Reynolds Number Hydrodynamics. Prentice-Hall, N. J.
9. Hirschfeld, B. R. 1972. Ph.D. Thesis. New York University. (Communicated through H. Brenner.)
10. Giddings, J. C., E. Kucera, C. P. Russell, and M. N. Myers. 1968. *J. Phys. Chem.* **72**:4397.
11. Spiegler, K. S., and O. Kedem. 1966. *Desalination.* **1**:311.
12. Anderson, J. L., and J. A. Quinn. 1972. *J. Chem. Soc. Faraday Trans. I.* **68**:608.
13. Bloomfield, V. A. 1968. *Science (Wash. D. C.)*. **161**:1212.
14. Pyun, C. W., and M. Fixman. 1964. *J. Chem. Phys.* **41**:937.
15. Tanford, C. 1961. Physical Chemistry of Macromolecules. John Wiley & Sons, New York.
16. Einstein, A. 1956. Investigations on the Theory of the Brownian Movement. R. Furth, editor. Dover Publications, New York.
17. Dubin, S. B., J. H. Lunacek, and G. B. Benedek. 1967. *Proc. Natl. Acad. Sci. U. S. A.* **57**:1164.
18. Conlon, T., and B. Craven. 1972. *Aust. J. Chem.* **25**:695.
19. Gladden, J. K., and M. Dole. 1953. *J. Am. Chem. Soc.* **75**:3900.
20. Reid, R. C., and T. K. Sherwood. 1958. Properties of Gases and Liquids. McGraw-Hill, New York. 284.
21. Gosting, L. J. 1956. *Adv. Protein Chem.* **11**:429.
22. Bearman, R. J. 1960. *J. Chem. Phys.* **32**:1308.
23. Goldsmith, H. L., and S. G. Mason. 1967. The Microrheology of Dispersions. *In* Rheology. Vol. 4. F. R. Eirich, editor. Academic Press, Inc., New York.
24. Goldman, A. J., R. G. Cox, and H. Brenner. 1967. *Chem. Eng. Sci.* **22**:637, 653.
25. Chow, T. S. 1973. *Phys. Fluids.* **16**:31.
26. Brenner, H., and P. M. Bungay. 1971. *Fed. Proc.* **30**:1565.

27. WANG, H., and R. SKALAK. 1969. *J. Fluid Mech.* **38**:75.
28. CHEN, T. C., and R. SKALAK. 1970. *Appl. Sci. Res.* **22**:403.
29. FERRY, J. D. 1936. *J. Gen. Physiol.* **20**:95.
30. KNUDSEN, J. G., and D. L. KATZ. 1958. Fluid Dynamics and Heat Transfer. McGraw-Hill, New York. 227.
31. LEVENSPIEL, O., and K. B. BISCHOFF. 1963. *Adv. Chem. Eng.* **4**:95.
32. SATTERFIELD, C. N., C. K. COLTON, and W. H. PITCHER, JR. 1973. *Am. Inst. Chem. Eng. J.* **19**:628.
33. BUNGAY, P. M. 1970. Ph.D. Thesis. Carnegie-Mellon University, Pittsburgh, Pa.
34. BECK, R. E., and J. S. SCHULTZ. 1970. *Science (Wash. D. C.).* **170**:1302.
35. UZELAC, B. M., and E. L. CUSSLER, JR. 1970. *J. Colloid Interface Sci.* **32**:487.
36. ANDERSON, J. L., and J. A. QUINN. 1972. *J. Colloid Interface Sci.* **40**:273.
37. MICHAELS, A. S. 1968. Ultrafiltration. *In* Progress in Separation and Purification. Vol. 1. E. S. Perry, editor. Interscience, New York.
38. KATCHALSKY, A., and P. F. CURRAN. 1965. Non-equilibrium Thermodynamics in Biophysics. Harvard University Press, Cambridge, Mass.
39. STAVERMAN, A. J. 1951. *Rech. Trav. Chim.* **70**:344.
40. SPIEGLER, K. S. 1958. *Trans. Faraday Soc.* **54**:1408.
41. DAINTY, J., and B. Z. GINZBURG. 1963. *J. Theor. Biol.* **5**:256.
42. BRENNER, H. 1970. *J. Fluid Mech.* **43**:641.
43. BRENNER, H. 1972. Suspension Rheology. *In* Progress in Heat and Mass Transfer. Vol. 5 W. R. Schowalter, editor. Pergamon Press, New York.